

© Du Zh., 2006.

Zh.Du

ENHANCEMENT OF POTASSIUM CURRENTS IN RAT DORSAL ROOT GANGLION NEURONS BY SULFUR DIOXIDE DERIVATIVES

Department of environmental science, Shanxi University of Finance & Economics,
Taiyuan 030006, PR China

Abstract

This study addressed the effect of sulfur dioxide (SO_2) derivatives on transient outward potassium currents (I_A and I_D) and delayed rectifier current (I_K) in somatic membrane of freshly isolated rat dorsal root ganglion neurons using the whole cell configuration of patch-clamp technique. SO_2 derivatives reversibly increased the amplitudes of potassium currents in a concentration-dependent and voltage-dependent. SO_2 derivatives significantly shifted the activation of delayed rectifier potassium current in the hyperpolarizing direction and shifted the inactivation curve of transient outward potassium currents in the depolarizing direction. Parameters for the fit of a Boltzmann equation to mean values for delayed rectifier current activation were $V_{1/2}=20.3\pm2.1$ mV before and 15.0 ± 1.5 mV after application $10\text{ }\mu\text{M}$ SO_2 derivatives. The half inactivation of I_A was shifted 6 mV and I_D 7.4 mV after application $10\text{ }\mu\text{M}$ SO_2 derivatives. These results indicated that SO_2 derivatives increased the amplitudes of potassium currents and changed the properties of potassium channels.

Keywords:

Sulfur dioxide derivatives; transient outward potassium currents; delayed rectifier current; Whole-cell patch clamp; Dorsal root ganglion

Introduction

Ion channels in cell membrane are targets for many toxins and drugs, more neuronal damaged are caused by interrupting the function of ion channels [4,17,24]. Neuronal membranes of dorsal root ganglion (DRG) neurons contain a variety of different voltage-operated potassium channels, which are especially important for the regulation of neuronal excitability [12,18]. In all investigated DRG neurons, whole-cell outward currents could be separated into three different components: fast inactivating (I_A), slow inactivating (I_D) and non-inactivating (I_K) potassium currents. I_A and I_D constitute transient outward potassium currents in this paper. One of the main functional properties of DRG neurons is relay function between sensors and central neurons. Each neuron in the DRG transduces synaptic input into a temporal code of action potentials, a code suitable for sending the information to other neurons of the spinal cord or to the central nucleus. DRG neurons can conduct high-frequency repetitive action potentials from the periphery to spinal cord motoneurons or to the central nucleus without significant delay. Outward potassium currents repolarize neuronal membranes in response to depolarizing events and stabilize the membrane potential. If the periphery nerve injury, these neurons often display aberrant firing properties that result in abnormal sensations [5,11].

Sulfur dioxide (SO_2) is a common air pollutant. Its derivatives, bisulfite and sulfite can be absorbed into blood or other body fluid [13,20]. SO_2 has been shown to exert various biological effects in both animals and plants [14,22,23]. SO_2 inhalation may cause changes of oxidative stress and antioxidation status in various organs of mice [14]. SO_2 inhalation can damage the brain of rats and guinea pigs

[10,22]. SO_2 or bisulfite-sulfite can bring about lipid peroxidation [15,16]. Lipid peroxidation is believed to be involved in several disease states, such as diabetes and neurodegenerative diseases as well as the aging process [3,21]. SO_2 derivatives can increase transient outward potassium currents in hippocampal CA3 neurons and sodium currents in DRG neurons of rats [7,8]. SO_2 derivatives have the vasodilatory effect on isolated aortic rings of rats, and explore the possible mechanism is correlated with K^+ flowing out. SO_2 inhalation can induce apoptosis of mouse spleen lymphocytes [2]. Now, we find that SO_2 derivatives induce DRG neurons apoptosis. Enhancement of outward potassium current can induce neuronal apoptosis [17,24]. So, it is of consequence to address the effect of sulfur dioxide on outward potassium currents in DRG neurons.

In the present study, we examined the effects of SO_2 derivatives on outward potassium currents in DRG neurons of rat in order probe into its possible mechanisms on nervous system.

Materials and methods

2.1 Cell preparation and electrophysiological recording

All experiments conformed to local and international guidelines on ethical use of animals and all efforts were made to minimize the number of animal used and their sufferings. 10~15 days postnatal Wistar rats, irrespective of sex, were rapidly decapitated. DRG neurons were isolated according to the method described in our previous study [8]. Medium size DRG neurons (30-40 μm in diameter) were used. Voltage-clamp recordings were made in the whole-cell patch-clamp technique at room temperature (20~25°C). Currents were recorded with Axopatch 200B patch clamp amplifier (Axon Instrument, USA), filtered at 2 kHz and stored in a computer using a digidata 1200B interface (Axon Instrument, USA) and Pclamp version 6.0.4 software (Axon Instrument, USA). The patch-clamp electrodes were pulled by a micropipette puller (Narishige, PP 830) with a tip resistance of 5~8 M Ω . The seal resistance was >1G Ω . Neurons with an inadequate seal were excluded from analysis. The

Contact Information:

Zhengqing Du

E-mail: duzhengqing@sxu.edu.cn

Tel: +86-351-7666169

Fax: +86-351-7666807

pipette solution contained (in millimolar concentrations): 10 KF, 4 NaCl, 130 KCl, 1 MgCl₂, 10 HEPES, 10 EGTA and 2 Na₂ATP, and the pH adjusted to 7.2 with tri (hydroxymethyl) aminomethane. The osmolarity was adjusted to 305 mosmol with sucrose. The external solution contained (in millimolar concentrations): 140 choline chloride, 4 KCl, 1 MgCl₂, 2 CaCl₂, 10 HEPES, 10 D-glucose, adjusted pH to 7.4 with NaOH.

The osmolarity was adjusted to 310 mosmol with sucrose. In this study, voltage-dependent Na⁺ channels were blocked by extracellular 1 μM TTX and Ca²⁺ channels were blocked by 100 μM CdCl₂. We dissolved 2.5 mM NaHSO₃ and 7.5 mM Na₂SO₃ in distilled water at a concentration of 10 mM derivatives (pH=7.4) and added it to the external solution just before each experiment. All chemicals unless otherwise specified were purchased from Sigma.

2.2 Drug applications and data analysis

Drug application was done using a "Y-tube method" and the outlet tip of Y-tube (0.1mm diameter) was set about 0.2mm away from the neuron under recording. The solution was applied to the Y-tube by vacuum pump. Data were analyzed using of pCLAMP CLAMPFIT procedures (Axon Instrument, USA) and Origin 5.0 software (Microcal software, USA). Results were presented as mean±S.D., and statistical comparisons were made using the paired Student's *t*-test, and probabilities less than 0.05 were considered significant. Dose-response curves were fitted with the Logistic equation of the form: $y = (A_1 - A_2) / [1 + (x/x_0)^p] + A_2$, where A_1 is initial value of SO₂ derivatives increase, A_2 is final value of

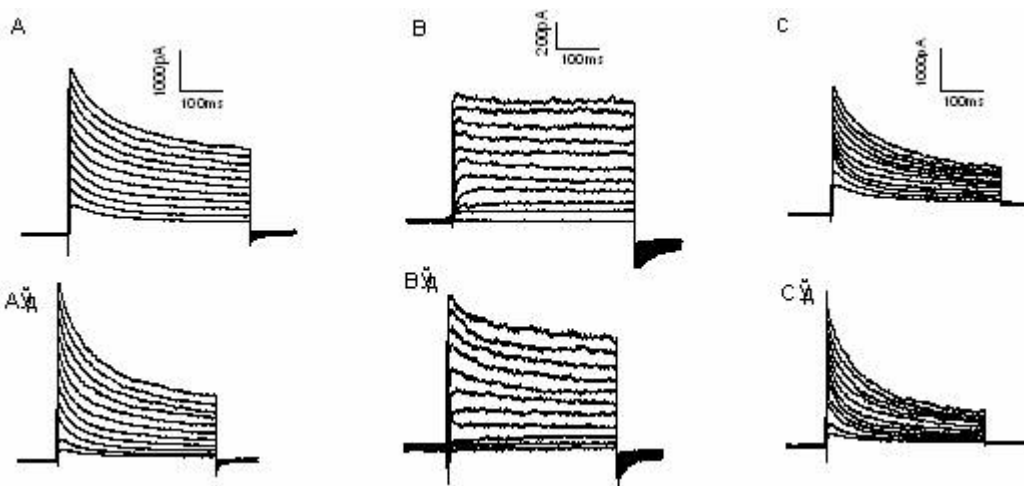


Fig.1. Outward potassium families elicited in acutely dissociated DRG neurons from rats at postnatal days of 10-15. (A) Potassium currents were evoked by 400 ms depolarization from -40 mV in increment of 10 mV up to +60 mV after the -120mV prepulse protocol. (B) Delayed rectifier potassium current were recorded from -40 mV to +60 mV from prepulse -40 mV. (C) Transient outward potassium currents elicited by subtracted of the record of B from A. (A', B', C') After the treatment of 10 μM SO₂ derivatives, the corresponding currents were increased.

SO₂ derivatives increase, x_0 is the center (IC₅₀ value), and p is the power. Activation curves and steady-state inactivation curves were fitted using the Boltzmann equation of the form: $I/I_{max} = [1 + \exp((V_{1/2} - V_c)/k)]^{-1}$, where I_{max} is the maximal current, $V_{1/2}$, the voltage at which the current is half activated or inactivated, and k is the slope factor describing the slope of the activation or steady-state inactivation curves.

Results

3.1 Outward potassium currents recording

Potassium currents were recorded using protocol shown in Fig.1A. The records were obtained by holding the resting potential at -80 mV. Activation of these currents was rapid to ensure that decay was only partial during a 400-ms depolarization pulse. Outward currents were elicited by stepping from -40 mV in increments of 10 mV up to +60 mV. Current at panel A was recorded after a 500-ms pre-conditioning pulse potential of -120 mV and panel B corresponds to a 500-ms pre-conditioning pulse potential of -40 mV. Thus we recorded all outward potassium currents in panel A and delayed rectifier currents in panel B. Currents elicited at panel C by the conditioning voltage were obtained by subtraction

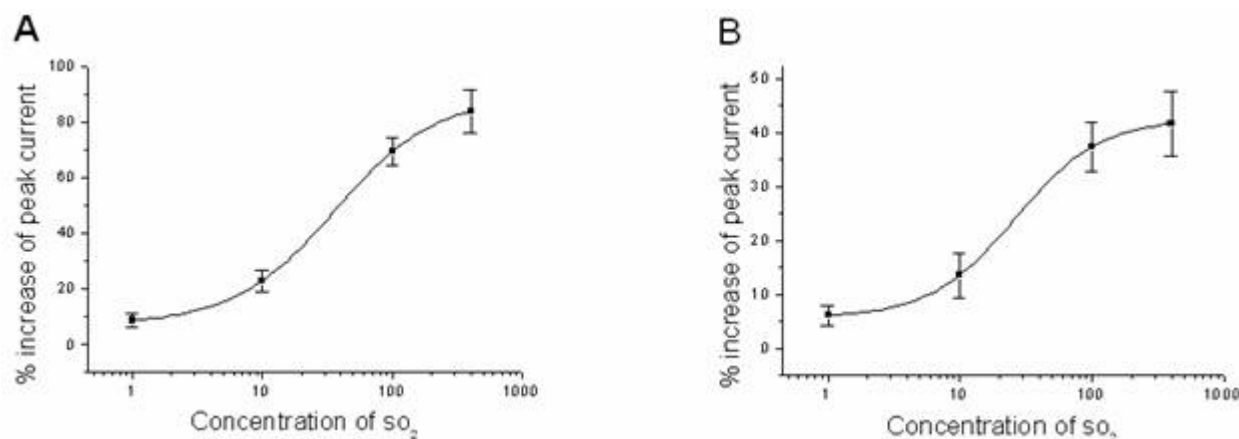


Fig.2. Dose-response curves for the effects of SO₂ derivatives on transient outward potassium currents (A) and delayed rectifier potassium current (B). Percent increment values were plotted against the SO₂ derivatives dose, fitted with the Hill function. Each point represents mean ± S.D. ($n = 15$)

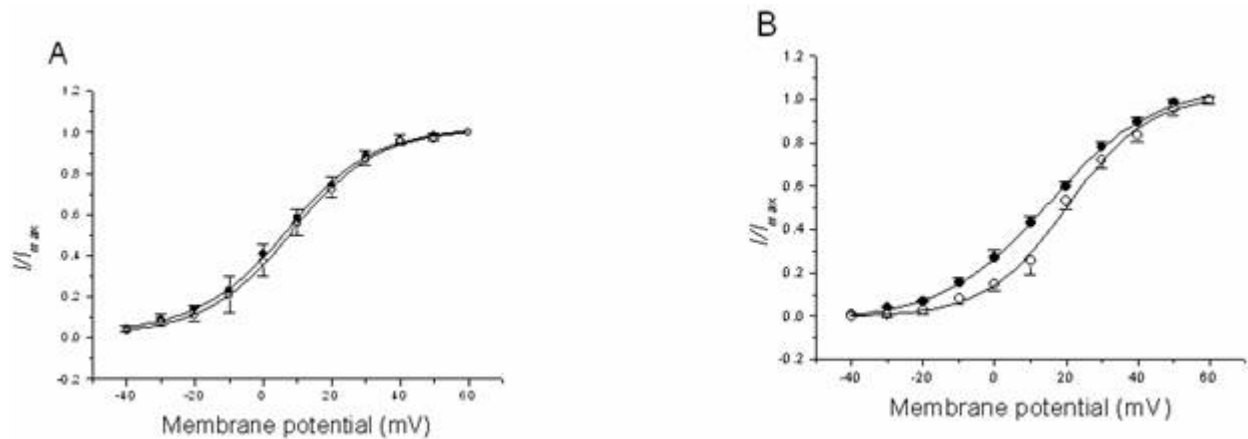


Fig.3 Effects of SO_2 derivatives on the activation curves of potassium currents. The curves were drawn according to the Boltzmann equation. \circ , control; \bullet , 10 μM SO_2 derivatives on transient outward potassium currents(A)and delayed rectifier potassium currents(B). (A, $n=15$; B, $n=13$)

of the -40 mV-prepulse current from the -120 mV-prepulse current. This is we record transient outward potassium currents in this paper. The amplitudes of potassium currents were enhanced by 10 μM SO_2 derivatives in every corresponding panel. It was come into view potassium currents partly recovered washing out the drug.

3.2 Concentration-dependent effect of SO_2 derivatives on potassium currents.

We recorded total potassium currents and delayed rectifier current in the solutions with 1, 10, 100, 400 μM SO_2 derivatives. The amplitude of transient outward potassium currents was respectively enhanced (8.6 \pm 2.3)%, (22.9 \pm 3.9)%, (69.4 \pm 5.1)%, (83.9 \pm 7.6)% with the four different concentrations of SO_2 derivatives. The delayed rectifier potassium currents were increased (6.1 \pm 1.9)%, (13.5 \pm 4.2)%, (37.3 \pm 4.6)%, (41.6 \pm 6.3)%, respectively. The enhanced effects were dose-dependent and voltage-dependent. As shown in Fig. 2, the dose-response curve of SO_2 derivatives at +60 mV was fitted with a Logistic equation. 50% enhanced concentration (EC_{50}) of SO_2 derivatives was about 35.8 μM in transient outward potassium currents and 26.3 μM in delayed rectifier current.

3.3 Effects of SO_2 derivatives on the activation of potassium channels.

The obtained transient outward potassium currents were plotted as a function of test depolarizing voltage steps. In the representative I - V curve transient outward potassium cur-

rents started to appear at more positive than -50 mV. The activation curve under the condition of control and exposure to 10 μM SO_2 derivatives were shown in Fig.3A. Each of the normalized curves was fitted with the single Boltzmann equation. In Fig.3A, there was a little shift to depolarized voltages of corresponding points of the normalized I - V curves at 10

μM SO_2 derivatives. Before and after application of 10 μM SO_2 derivatives, the values of $V_{1/2}$ were 8.2 \pm 1.5 mV and 6.9 \pm 1.1 mV ($n=15$, $P>0.05$), respectively, with k of 12.8 \pm 0.9 mV and 12.9 \pm 0.9 mV ($n=15$, $P>0.05$), respectively. In delayed rectifier currents the Boltzmann function was best fitted to the data and the membrane potential for the half-maximum current was estimated to be 20.3 \pm 2.1 mV and the slop factor was 11.3 \pm 0.6mV in absence of SO_2 derivatives. After 10 μM SO_2 derivatives application, these values were 15.0 \pm 1.5 mV and 14.6 \pm 1.2mV, respectively, the difference was statistically significant (Fig. 3B).The results showed that 10 μM SO_2 derivatives only affected the activation process of delayed rectifier potassium current.

3.4 Effects of SO_2 derivatives on the inactivation of transient outward potassium channels.

Transient outward potassium currents include two differ-

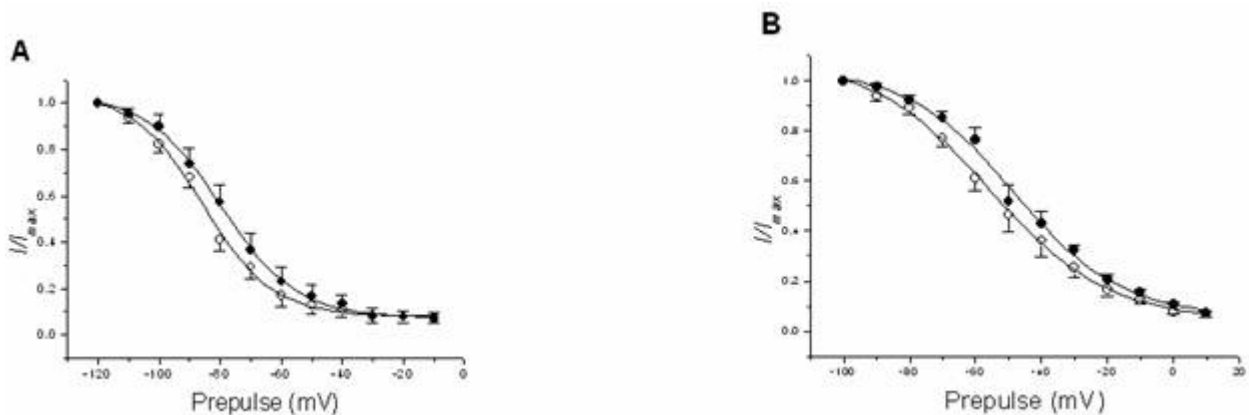


Fig.4. Effects of SO_2 derivatives on steady-state inactivation curves for I_A and I_D . The current amplitude was normalized to the maximum current amplitude. The curves were drawn according to the Boltzmann equation. \circ , control; \bullet , 10 μM SO_2 derivatives on I_A (4A) and I_D (4B)

ent components: fast inactivating (I_A) and slow inactivating (I_D). The steady-state inactivation of I_A was recorded by a double-pulse protocol, 80ms hyperpolarizing or depolarizing prepulse from -120mV to +10mV were followed by a 400-ms test depolarization to +60mV. The inactivation of I_D was studied with 1s hyperpolarizing prepulses from -100mV to +10mV (10mV steps), followed by a 500ms depolarizing pulse to 0mV. Currents at the end of the depolarizing pulse were determined as I_D .

The inactivation curves shown in Fig. 4 were obtained by normalizing the test current amplitudes by taking the maximum value under each condition as unity. The curves were well fitted with the Boltzmann function. Application of SO_2 derivatives resulted in a depolarizing shift of the steady state inactivation curve for both the K^+ currents. During control conditions, $V_{1/2}$ for inactivation of I_A in control and SO_2 derivatives 10 μM were -85.7 ± 5.1 mV and -79.7 ± 2.6 mV ($n = 15$, $P < 0.05$ vs. control), with k of 11.4 ± 0.8 mV and 12.3 ± 1.47 mV ($n = 15$, $P > 0.05$ vs. control), respectively. And $V_{1/2}$ for inactivation of I_D in control was -55.7 ± 2.1 mV and -48.3 ± 1.9 mV after application 10 μM SO_2 derivatives ($n = 11$, $P < 0.01$ vs. control), with k of 17.9 ± 1.0 and 16.2 ± 0.97 mV ($n = 12$, $P > 0.05$ vs. control), respectively.

3.5 Effects of SO_2 derivatives on the time-dependent kinetics

To further investigate the effects of SO_2 derivatives on activation kinetics and inactivation kinetics of potassium currents, we studied the time to reach the peak of current (t) and time constants of inactivation (τ).

For transient outward potassium currents, time to peak was not changed before and after application of 10 μM SO_2 derivatives. The t value were 4.4 ± 0.25 ms and 3.9 ± 0.23 ms ($n = 12$, $P > 0.05$) in the presence of SO_2 derivatives, respectively. However, the decay time constant was markedly prolonged by SO_2 derivatives. The inactivation time constant changed from 18.4 ± 3.2 to 27.4 ± 4.5 ms at +60mV ($n = 10$, $P < 0.01$) in I_A and changed from 186.7 ± 12.2 ms to 256.61 ± 18.9 ms at +60mV ($n = 10$, $P < 0.01$) in I_D after application SO_2 derivatives. For I_K , time to peak was decreased by 10 μM SO_2 derivatives significantly. The t value were 36.0 ± 5.01 and 21.7 ± 2.47 ms ($n = 10$, $P < 0.01$). These results indicated that SO_2 derivatives delayed the inactivation of transient outward potassium currents, accelerated the activation of delayed rectifier potassium current.

Discussion

The present study indicated that SO_2 derivatives significantly increased outward potassium currents in rat dorsal root ganglion neurons. Besides the increase of transient outward potassium currents and delayed rectifier potassium currents, SO_2 derivatives also affected gating kinetics of delayed rectifier potassium currents to more negative potentials. Next, SO_2 derivatives significant shifted the steady-state inactivation curve of I_A and I_D to the positive direction.

SO_2 derivatives did not change transient outward potassium currents activation potential, this would not affect the excitability of DRG neurons. SO_2 derivatives caused a positive shift of the inactivation curves. The effect would in-

crease the excitability of DRG neurons. So the final result was that SO_2 derivatives increased the excitability of DRG neurons. Transient outward potassium currents are thought to modulate the timing of repetitive action potential generation, and the time required to reach the threshold to fire an action potential [1,6,9,19]. After SO_2 derivatives application, the DRG neurons kept a continuance of depolarize, prolong the time of action potential, facilitated energy expenditure. Thus, these neurons might display aberrant firing properties that resulted in abnormal physiological characteristic. This variation caused by SO_2 derivatives may be took an important part in excitotoxic effects on the periphery neural system. SO_2 derivatives enhanced the delayed rectified potassium currents, promoted the activation process. So the final result was that SO_2 derivatives increased K^+ efflux from potassium channels and increased membrane K^+ permeability. Augmentation in delayed rectifier potassium currents and loss of neuronal cell K^+ occurred early in the course of neuronal apoptosis [17,24]. In addition, the non-inactivating delayed rectifier potassium current augmentation was specific to apoptosis but not triggered by necrotic insult or in older cell resistant to apoptosis [24]. So, SO_2 derivatives significantly increasing delayed rectifier potassium current may be a primary step leading to apoptosis of DRG neurons.

The neurotoxic effects of SO_2 on potassium channels are studied here. These results suggested that SO_2 derivatives increased the excitability of DRG neurons by changing the property of transient outward potassium channels; SO_2 derivatives induced vital DRG neurons apoptosis by increasing the conductance of delayed rectifier potassium channel and increasing membrane K^+ permeability.

Concerning the SO_2 poisoning, the effects of SO_2 on potassium channels have to be taken into consideration as a possible contributing mechanism for the neurological symptoms of enhanced neuronal activity and induced neurons apoptosis seen during severe SO_2 intoxication.

Acknowledgements

This work was supported with National Basic Research Program of China (G30230310), National Nature Science Foundation of China (No.30070640).

References

1. G.K. Aghajanian, Modulation of a transient outward current in serotonergic neurons by $\alpha 1$ -adrenoceptors, *Nature*, 315(1985) 501-503.
2. J.Y. Bai, Z.Q. Meng, The relationship between GSH and apoptosis of mouse spleen lymphocytes induced by SO_2 . *Journal of Health Toxicity*, 17(2003)42-44
3. J.W. Baynes, Role of oxidative stress in development of complications in diabetes, *Diabetes*, 40(1991)405-412.
4. P. Calabresi, A. Pisani, N.B. Mercuri, G. Bernardi, On the mechanisms underlying hypoxia-induced membrane depolarization in striatal neurons, *Brain*, 118(1995)1027-1038.
5. M. Devor, P.D. Wall, Cross-excitation in dorsal root ganglia of nerve-injured and intact rats, *J. Neurophysiol.* 64(1990)1733-1746.
6. M.M. Dourado, S.E. Dryer, Regulation of A-currents by cell-cell interactions and neurotrophic factors in developing chick parasympathetic neurons, *J. Physiol.* 474(1994)367-377.
7. Z.Q. Du, Z.Q. Meng, Modulation of sodium currents in rat dorsal root ganglion neurons by sulfur dioxide derivatives, *Brain Res.* 1010(2004)127-133.
8. Z.Q. Du, Z.Q. Meng, Effects of Derivatives of sulfur dioxide on Transient Outward Potassium Currents in Acutely Isolated Hippocampal Neurons, *Food and chemical toxicology*. 42 (2004)1211-1216.
9. S.K. Florio, M.R. Vasko, R.J. Bauer, J.L. Kenyon, Transient potassium currents in avian sensory neurons, *J. Neurophysiol.*

- 63(1990)725-737.
10. S.S. Haider, M. Hasan, S.N. Hasan, S.R. Khan, S.F. Ali, Regional effects of sulfur dioxide exposure on the guinea pig brain lipids, lipid peroxidation and lipase activity, *Neurotoxicology*. 2 (1981) 443-450.
 11. K.C. Kajander, S. Wakisaka, G.J. Bennett, Spontaneous discharge originates in the dorsal root ganglion at the onset of a painful peripheral neuropathy, *Neurosci. Lett.* 138(1992) 225-228.
 12. S.A. Matin, J.M. Nerbonne, Elimination of the fast transient in superior cervical ganglion neurons with expression of KV4.2W362F: molecular dissection of I_A , *J. Neurosci.* 20(2000) 5191-5199.
 13. Z.Q. Meng, B. Zhang, Polymerase chain reaction-based deletion screening of bisulfite (sulfur dioxide)-enhanced gpt-mutants in CHO-AS52 cells, *Mutat. Res.* 425(1999)81-85.
 14. Z.Q. Meng, Oxidative damage of sulfur dioxide on various organs of mice: sulfur dioxide is a systemic oxidative damage agent, *Inhal Toxicol.* 15(2003) 181-195.
 15. Z.Q. Meng, L. Zhang, Chromosomal aberrations and sister-chromatid exchanges in lymphocytes of workers exposed to sulphur dioxide, *Mutat. Res.* 241(1990)15-20.
 16. Z.Q. Meng, L. Zhang, Cytogenetic damage induced in human lymphocytes by sodium bisulfite, *Mutat Res.* 298(1992)63-69.
 17. S. Pal, K.A. Hartnett, J.M. Nerbonne, E.S. Levitan, E. Aizenman, Mediation of neuronal apoptosis by $K_v2.1$ -encoded potassium channels, *J. Neuroscience*, 23(12)(2003)4798-4802.
 18. B. Rudy, A. Chow, D. Lau, Y. Amarillo, A. Ozaita, M. Saganich, H. Moreno, M.S. Nadal, P.R. Hernandez, C.R. Hernandez, A. Erisir, C. Leonard, M.E. Vega-Saenz, Contributions of K_v3 channels to neuronal excitability, *Ann. N. Y. Acad. Sci.* 868 (1999) 304-343.
 19. P. Serodio, C. Kentros, B. Rudy, Identification of molecular components of A-type channels activating at subthreshold potentials, *J. Neurophysiol.* 72(1994)1516-1529.
 20. R. Shapiro, Genetic effects of bisulfite (sulfur dioxide). *Mutat. Res.* 38(1977)149-176.
 21. A.L. Tappel, H. Zalkin, Inhibition of lipid peroxidation in microsomes by vitamin E, *Nature*, 185(1960)35-43.
 22. P. Yargicoglu, A. Agar, S. Gumuslu, S. Bilmen, Y. Oguz, Age-related alterations in antioxidant enzymes, lipid peroxide levels, and somatosensory-evoked potentials: Effect of sulfur dioxide, *Arch. Environ. Contam. Toxicol.* 37(1999)554-560.
 23. H.L. Yi, Z.Q. Meng, Genotoxicity of hydrated sulfur dioxide on root tips of allium sativum and vicia faba, *Mutation Res.* 537 (2003)109-114.
 24. S.P. Yu, C.H. Yeh, S.L. Sensi, B.J. Gwag, L.M.T. Canzoniero, Z.S. Farhangrazi, H.S. Ying, M. Tian, L.L. Dugan, D.W. Choi, Mediation of neuronal apoptosis by enhancement of outward potassium current, *Science*. 278(1997) 114-117.

© Farasyn A, Meeusen R. , 2006.

A.Farasyn , R.Meeusen

VALIDITY OF THE NEW BACKACHE INDEX (BAI) IN PATIENTS WITH LOW BACK PAIN

Fac. LO & Rehab., Free Univeristy Brussels (VUB)
Belgium

ABSTRACT.

Background context: The Backache-Index (BAI) is applied to patients with low back pain (LBP) in order to help the doctors/surgeons perform physical examinations easily and it is carried out within a short space of time (< 2 min.) without using inclinometric instruments.

Purpose: To explore the reliability, validity and responsiveness of this new Backache-Index in patients with low back pain, which can fulfil the existing need for a reliable routine examination in the clinical environment.

Study design/setting: Patients with LBP filled in disability questionnaires, pain rating scales and physical impairment tests were completed in function of construct validity and correlation studies. A subgroup was evaluated for inter-observer and test-retest reliability and a second group was reassessed after two active treatment sessions in order to verify the responsiveness compared with other examined variables.

Patient sample: In total, 75 patients with subacute LBP (3-12 weeks) participated in a randomized controlled study.

Outcome measures: The validity of the BAI was explored through a correlation with the standard Oswestry LBP Disability Index (ODI), the McGill LBP Questionnaire Index (MPQ), and the Visual Analogue Scale (VAS).

Methods: The BAI consisted of a scoring system that includes pain factors and stiffness estimation at the end of a series of five different lumbar movements of a patient standing in an erect position.

Results: The correlations between the separate outcomes and the BAI ranged from 0.61 to 0.76 ($P < 0.001$). The inter-observer reliability between two experienced observers for the 5 outcome scores was good ($ICC > 0.86$) and even perfect for the BAI ($ICC = 0.96$). A BAI change of one unit is able to exclude a measurement error. A significantly good correlation ($P < 0.001$) was found between the BAI at baseline, and the ODI ($R = 0.62$) and the MPQ-PRIT, as the total degree of pain rating index ($R = 0.57$), a moderate correlation with the MPQ-NWCT, as the total number of chosen adjectives from the whole list of adjectives ($R = 0.48$) and the VAS ($R = 0.47$), but a lower correlation was found with the MPQ-Quality of life index ($R = 0.43$). The effect size and discriminative ability of the measures were explored after two treatment sessions of deep transverse friction myotherapy by means of the study of the receiver operating characteristics curve (ROC) and the greatest area under the curve (AUC). The greatest level of distinction was found for the MPQ-PRI-T and the BAI ($AUC > 0.93$), followed by the ODI ($AUC = 0.92$). A lower level of distinction was found for the MPQ-NWC-T and the VAS ($AUC > 0.82$).

Conclusions: The Backache Index or BAI appears to be a reliable and valid assessment of overall restricted spinal movements in case of LBP and discriminates between successful and unsuccessful treatment outcome.

Keywords:

Low back pain – outcome scales - reliability - validity – responsiveness- impairment – pain rating scales.